American Journal of Pathology, Vol. 161, No. 3, September 2002

Inhibition of Prostate Tumor Cell Hyaluronan Synthesis Impairs Subcutaneous Growth and Vascularization in Immunocompromised Mice

Melanie A. Simpson,* Christopher M. Wilson,* and James B. McCarthy*†

From the Department of Laboratory Medicine and Pathology and the University of Minnesota Cancer Center,† University of Minnesota, Minneapolis, Minnesota*

Hyaluronan (HA), a secreted glycosaminoglycan component of extracellular matrices, is critical for cellular proliferation and motility during development. However, elevated circulating and cell-associated levels correlate with various types of cancer, including prostate. We have previously shown that aggressive PC3M-LN4 prostate tumor cells synthesize excessive HA relative to less aggressive cells, and express correspondingly higher levels of the HA biosynthetic enzymes HAS2 and HAS3. Inhibition of these enzymes by stable transfection of PC3M-LN4 cells with antisense HAS2 or HAS3 expression constructs diminishes HA synthesis and surface retention. In this report, we used these HA-deficient cell lines to examine the role of HA in tumorigenicity. Subcutaneous injection of SCID mice with hyaluronan synthase (HAS) antisense-transfected cells produced tumors threefold to fourfold smaller than control transfectants. Tumors from HAS antisense transfectants were histologically HA-deficient relative to controls. HA deficiency corresponded to threefold reduced cell numbers per tumor, but comparable numbers of apoptotic and proliferative cells. Percentages of apoptotic cells in cultured transfectants were identical to those of control cells, but antisense inhibition of HA synthesis effected slower growth rate of cells in culture. Quantification of blood vessel density within tumor sections revealed 70 to 80% diminished vascularity of HAS antisense tumors. Collectively, the results suggest HAS overexpression by prostate tumor cells may facilitate their growth and proliferation in a complex environment by enhancing intrinsic cell growth rates and promoting angiogenesis. Furthermore, this is the first report of a role for inhibition of HA synthesis in reducing tumor growth kinetics. ***(Am J Pathol 2002, 161:849–857)***

Prostate cancer is the second leading cause of cancer death in men.[1] In prostate cancer progression, prostate epithelial cells undergo phenotypic and genotypic changes that facilitate inappropriate proliferation, invasion of surrounding stromal matrices, entry into the lymphatic system and/or the bloodstream, and colonization of other tissues in the body. Understanding the molecular events that mediate these processes is essential to ultimate disease diagnosis, management, and treatment.

Hyaluronan (HA) is a secreted glycosaminoglycan abundant in stromal matrices and important for providing cushion around organ tissue and within joints.[2] However, more active roles for HA have been demonstrated in proliferation, in which its deposition facilitates rounding of mitotic cells;[3] development, in which it is both a scaffold for the movement of differentiating cells and a stimulus for the transformation to a mesenchymal phenotype that precedes cellular migration to form organs such as the heart[4] and prostate;[5] and wound healing, in which accelerated synthesis serves to recruit lymphocytes to the wound through the action of specific HA receptors.[6] Because these functions for HA are also components of aggressive tumor cell behavior, it is not surprising that HA has been implicated in tumorigenicity and metastasis. In fact, HA overproduction is a diagnostic or prognostic factor for several types of cancer, including breast,[7] thyroid,[8] ovarian,[9] colorectal,[10] and bladder cancers.[11] In histopathological analyses of human prostate cancer,[12–14] excessive stromal HA accumulation is detectable in early stages and intensifies throughout progression. Eventually, advanced cancers exhibit tumor cell-associated HA, which correlates to poor patient prognosis.[15]

HA biosynthesis is catalyzed by transmembrane HA synthase (HAS) enzymes.[16] Three human isozymes have been identified and cloned (*has1*,[17] *has2*,[18] *has3*[19]). The cDNA of each isozyme is capable of conferring HA synthesis and pericellular HA retention to transfected cells, and the HA products and rates of synthesis seem to be

Supported by funds from the United States Army Medical Research and Material Command (grants DA/DAMD 17-99-A-9029 and DA/DAMD 17-02-1-0102) and a National Institutes of Health National Research Service Award postdoctoral fellowship 1F32-CA84619-02 (to M. A. S.).

Accepted for publication May 15, 2002.

Present address for Melanie A. Simpson is the Department of Biochemistry, University of Nebraska, Lincoln, NE.

Address reprint requests to Dr. James B. McCarthy, Department of Laboratory Medicine and Pathology, University of Minnesota, Mayo Mail Code 609, 420 Delaware St. S.E., Minneapolis, MN 55455. E-mail: mccar001@tc.umn.edu.

very comparable in these transfectants.[20,21] Manipulation of specific isozyme expression levels has been demonstrated to affect tumorigenicity and metastasis. Overexpression of HAS2 in fibrosarcoma cells or HAS3 in prostate carcinoma cells yields significantly larger subcutaneous tumors in nude mice.[22,23] These results suggest involvement of HA in tumor growth, and imply that specific HAS isozymes and/or expression levels of those isozymes may mediate this process.

Previous work in our laboratory has been directed at determining the role of HA biosynthetic enzymes in prostate cancer. Initially, we demonstrated overexpression of mRNA for HAS isozymes 2 and 3 in PC3M-LN4, an aggressive prostate carcinoma cell line,[24] relative to less aggressive prostate tumor cell lines and normal prostate.[25] Overexpression of HAS2[22] and HAS3[23] has been shown to enhance growth of human tumor cell transfectants in immunocompromised mice, but the effect of inhibited HA production by tumor cells has not been determined. Altered HA synthesis and/or pericellular HA retention by prostate carcinoma cells could contribute to tumorigenic behavior, either by overall HAS expression level or in an isozyme-specific manner. Seeking to establish a functional correlation, we developed and characterized four stably transfected PC3M-LN4 cell lines.[26] An appropriate vector control; H2as, expressing only HAS2 antisense; H3as, with HAS3 antisense only; and H2/3as, a double knockout incorporating antisense for both HAS2 and HAS3. Significant inhibition of HA synthesis and pericellular HA retention was obtained by stable transfection with individual HAS antisense, with double antisense transfectants most dramatically affected.[26]

In this study, our goal was to evaluate the impact of inhibited HA production on prostate tumor cell growth in an animal model. We found the presence of excessive HA was required for efficient tumor growth, and investigated the potential mechanisms by which growth kinetics were altered. Apoptosis was unaffected either in tumor sections or cultured cells. The intrinsic rate of proliferation in culture was modestly reduced by HAS antisense inhibition, although the absolute percentage of proliferating cells within the tumor sections was not impacted. Quantification of blood vessel density among the cell lines revealed significantly reduced vascularization of HAS antisense-inhibited transfectant tumors. We conclude that the role of HA in prostate tumor cell biology is both proliferative and angiogenic.

Materials and Methods

Cell Culture and Reagents

The PC3-derivative cell line, PC3M-LN4 (human prostate adenocarcinoma cells), was kindly provided by Dr. Isaiah J. Fidler (M. D. Anderson Hospital Cancer Center, Houston, TX), and was maintained in minimal essential medium containing 10% fetal bovine serum, sodium pyruvate, and nonessential amino acids. Media supplements, and antibiotics were purchased from Invitrogen (Carlsbad, CA). Stably transfected cells selected as previously described[26] were maintained in the above medium containing 1 mg/ml of G418 and 0.5 mg/ml of hygromycin until one passage before injection, at which time this medium was replaced with standard medium. C.B-17.scid mice were purchased from Charles River, Wilmington, MA.

Mouse Subcutaneous Injection and Analysis

Male SCID mice (five animals per condition in three separate experiments) were injected subcutaneously in each flank with 1×10^6 tumor cells suspended at 10×10^6 cells/ml in standard culture medium. Tumor growth was monitored every 3 to 7 days using digital calipers. After 21 days, mice were sacrificed, a final caliper reading was recorded, and tumors were dissected and weighed. One part of each tumor was snap-frozen in OCT compound on dry ice for subsequent sectioning and CD31 detection. The other part was formalin-fixed, paraffin-embedded, and sectioned for histological analysis. Five sections per tumor type were stained with hematoxylin and eosin (H&E).

Detection of HA in Tumor Sections

HA was specifically detected in tumor sections with a biotinylated HA-binding protein (Seikagaku) at 3 μg/ml in phosphate-buffered saline (PBS)/1% bovine serum albumin overnight at 4°C. Sections were then washed, incubated for 1 hour with avidin-horseradish-peroxidase conjugate (Vector Laboratories, Irvine, CA), developed with the 3,3′-diaminobenzidine tetrahydrochloride liquid substrate system (Sigma Chemical Co., St. Louis, MO) for 10 minutes, hematoxylin-counterstained, and examined microscopically for 3,3′-diaminobenzidine tetrahydrochloride deposition.[15] Representative sections were digitally photographed at $\times$400 magnification.

Cellularity Determination

Cell counts were determined manually in hematoxylin-stained frozen sections. Five random sections were counted in each of four to five tumors per cell line and averages plotted in a distribution with the mean represented by a horizontal bar. To obtain relative cell numbers per tumor, the average two-dimensional cell counts were integrated to a three-dimensional volumetric density and normalized to the average three-dimensional volume of each tumor.

Apoptosis

Subconfluent cultures of equivalent passages of tumor cell lines were trypsin released, washed twice in PBS, and fixed/permeabilized by addition of ice-cold ethanol. Control aliquots of each cell suspension were incubated with 10 μg/ml of DNase. A terminal dUTP nick-end labeling (TUNEL) assay for DNA fragmentation, an early event in apoptosis, was performed according to the manufac-

turer's protocols using the TUNEL-Red apoptosis detection kit from Boehringer Mannheim, Indianapolis, IN. Cells were analyzed by two-color flow cytometry, gating on GFP-positive cells, and assessing incorporation of the red fluorophore in the FL-2 channel.

Intrinsic Growth Rate

Equivalent passages of each tumor cell line were plated at 2000 cells/well in 48-well plates. At 24-hour intervals up to 6 days, quadruplicate wells of each cell line were released with 150 μl of trypsin, neutralized with 150 μl of serum-containing medium, and manually counted in a hemacytometer.

Angiogenesis Quantification

Vascularization of the tumors was assessed in acetone-fixed frozen sections by antibody staining for CD31, a transmembrane protein specifically expressed by vascular endothelial cells. CD31-phycoerythrin-conjugated antibody (BD Pharmingen) staining was visualized by fluorescence microscopy. Five random sections from each of three tumors per cell line were digitally photographed with 5 seconds of exposure time, saved as TIF files, and processed as previously described.[27] Briefly, images were converted from 16 bit to 8 bit in Adobe Photoshop, red channel fluorescence was specifically isolated, images were converted to grayscale, inverted, and a black-and-white threshold was arbitrarily set to 200 based on levels. The histogram function was then used to determine vessel density as represented by density of black pixels at 0 on the black-to-white scale. Average pixel density for each transfectant tumor section was normalized to the average pixel density for untransfected PC3M-LN4 tumor sections.

Subcutaneous Injection with Exogenous HA

Tumor cells (GFP control and H2/3as cell lines) were resuspended in standard culture medium as above or in medium containing 1 mg/ml of sodium hyaluronate (average molecular size 810 kd; Lifecore, Chaska, MN), solubilized overnight, and filter-sterilized. Male SCID mice (five per condition in two separate experiments) were injected subcutaneously in each flank and monitored as above.

Results

Inhibition of Hyaluronan Synthase (HAS) by Anti-Sense RNA Expression Reduces Growth Rate of Subcutaneous Tumors

In a previous report, we described four stably transfected subline populations of PC3M-LN4 prostate adenocarcinoma cells: GFP, bearing the appropriate vector controls; H2as, expressing HAS2 antisense; H3as, with HAS3 antisense only; and H2/3as, incorporating antisense for both HAS2 and HAS3.[26] To evaluate the relevance of tumor cell HA to tumor growth *in vivo*, we performed subcutaneous injections of PC3M-LN4 untransfected cells, control vector-transfected cells, or stable HAS antisense-inhibited transfectants, into flanks of male SCID mice. At 3 weeks after injection, mice were sacrificed, and tumors were dissected and weighed. All tumors appeared encapsulated and no spontaneous metastasis was detected in any of the animals. Vector-transfected control cells formed tumors of comparable size to those of PC3M-LN4-untransfected cells (Figure 1). Expression of either antisense HAS2 or HAS3 individually, or in concert, in these cells, however, reduced the size of resultant tumors by 70 to 75%, suggesting HA overproduction was required for rapid tumor growth.

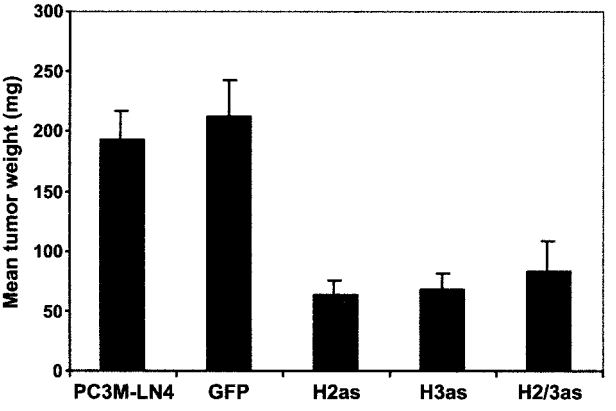

Figure 1. Inhibition of HAS gene expression in PC3M-LN4 cells by stable transfection with antisense constructs impairs tumor growth kinetics in immunocompromised mice. Untransfected, or vector (GFP)-, HAS2 (H2as)-, HAS3 (H3as)-, and HAS double antisense (H2/3as)-transfected tumor cells were suspended in serum-containing medium and injected subcutaneously into the flanks of male SCID mice. Tumors were harvested and weighed after 3 weeks. Data are plotted as the mean tumor wet weight (mg) ± SEM of 10 tumors per condition and are representative of three separate experiments.

Tumors Derived from HAS Antisense-Expressing Cells Contain Reduced HA and Diminished Cell Counts

H&E staining of tumor sections derived from control and transfected PC3M-LN4 cells confirmed the encapsulated, locally confined nature of the tumors. There was no evidence of necrosis, invasiveness, or spreading in any of the sections, and no apparent differences in morphology among cell lines. GFP expression within the transfectant tumor sections was verified by antibody staining (data not shown). To assess HA content of subcutaneous PC3M-LN4 tumors, formalin-fixed, paraffin-embedded tumors were sectioned, dewaxed, and probed with biotinylated HA-binding protein. HA appeared as a heavy brown stain interspersed among purple hematoxylin-counterstained tumor cells (Figure 2A). HA content and specificity of the probe was verified by absence of stain when sections were pretreated with hyaluronidase enzyme (Figure 2B). HA content of subcutaneous PC3M-LN4 transfectant tumors was then evaluated and visualized (Figure 2; C to F). As illustrated by the representative

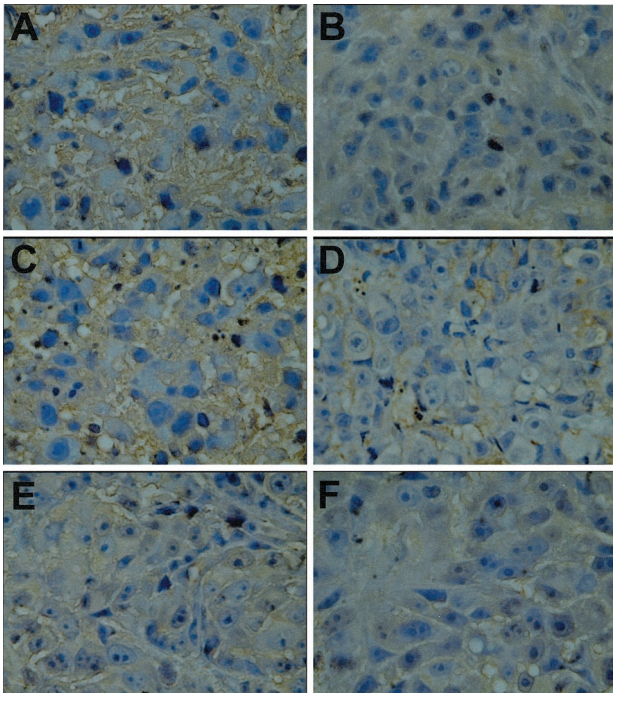

Figure 2. Evaluation of tumor HA content. Formalin-fixed paraffin-embedded sections were dewaxed, rehydrated, hematoxylin-stained, and probed with biotinylated HA-binding protein. After incubation with streptavidin-horseradish peroxidase conjugate, HA was detected by 3,3′-diaminobenzidine tetrahydrochloride precipitation. Representative stained tumor sections from each cell line are shown at ×400 magnification: **A:** PC3M-LN4; **B:** PC3M-LN4, hyaluronidase-treated; **C:** GFP control; **D:** H2as; **E:** H3as; **F:** H2/3as.

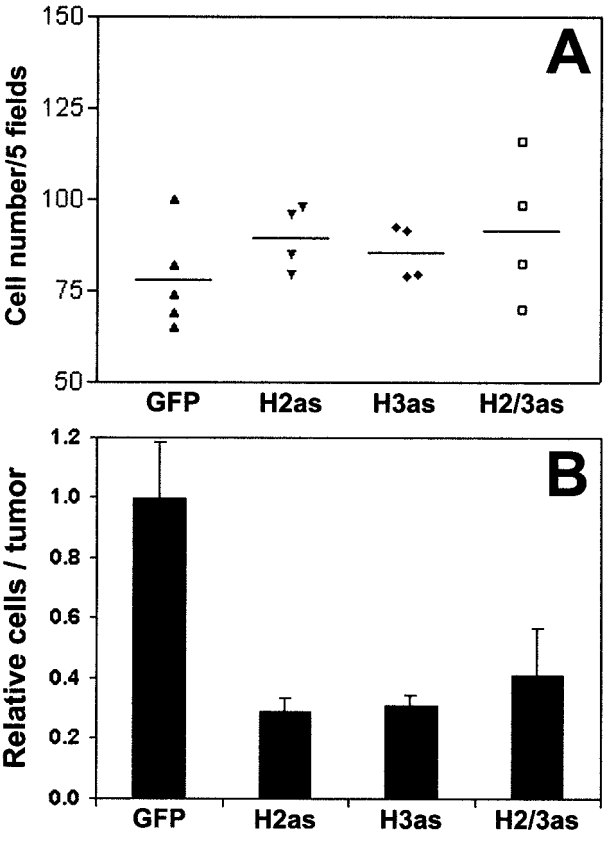

Figure 3. Cell counts in HAS antisense tumors. **A:** Individual cells in hematoxylin-stained frozen sections were manually counted under ×400 magnification and the average number of cells per five random fields was determined. Results of four to five tumors per cell line are plotted as a distribution with the mean represented by a **horizontal bar**. **B:** Two-dimensional average cell densities were integrated to volume densities, normalized to tumor size, and plotted as the mean relative fractional cell number ± SEM.

sections presented, GFP control tumors (Figure 2C) were similarly HA-rich, relative to the untransfected tumors, but individual or double HAS antisense tumors contained little to no intercellular HA (Figure 2; D, E, and F), consistent with reduced production by the tumor cells.

Because massively reduced intercellular HA within the tumors could translate to smaller tumor volumes with equivalent cell numbers, we quantified cellular density of the tumor sections. Cells were manually counted in five random hematoxylin-stained sections from four to five tumors for each cell line. Two-dimensional cell densities (Figure 3A) were only slightly greater in the antisense tumors. However, integration to three dimensions using the relative volumes of the respective tumors (Figure 3B) illustrated 2.5- to 3-fold more cells in control tumors. Hence although cell densities were somewhat increased by the absence of HA within the antisense tumors, the difference in tumor size was primarily the result of reduced cell number.

HAS Antisense Expression Reduces Intrinsic Growth Rate of PC3M-LN4 Cells But Does Not Affect Apoptosis or Proliferation Rate in Tumors

Cell counts in locally confined tumors are the result of a balance between apoptosis and growth in the tumor cell populations. Apoptosis was measured by a TUNEL assay for DNA fragmentation in fixed, permeabilized tissue sections. Sections viewed by fluorescence microscope exhibited virtually no apoptotic cellular staining (data not shown). However, at 3 weeks within the subcutaneous environment, apoptosis may no longer be detectable by this method, so we repeated the assay on cultured cell suspensions. Results were analyzed by flow cytometry (Figure 4; A to D), gating on GFP-positive cells, and detecting red fluorophore incorporation by apoptotic cells in FL-2 (black tracings). Approximately 1 to 2% of the GFP-positive cells were undergoing apoptosis and no differences in this percentage were evident among cell lines. DNase treatment of permeabilized cells was included as a control (gray tracings). Similar results were obtained by annexin-V staining (3 to 4% of GFP-positive cells were annexin-V-positive in all cell lines, data not shown), suggesting inhibition of HA production did not stimulate apoptosis in stably selected cultures.

Intrinsic growth rate of cells in culture was monitored by trypsin release and manual counting each day for 6 days (Figure 4E). Growth of individual HAS antisense transfectants was moderately impaired, and double antisense cell growth rate was 60% of control in the 6-day assay. We evaluated proliferation within tumor sections by staining for the nuclear proliferation antigen Ki-67 (not shown). The average percentage of Ki-67-positive cells

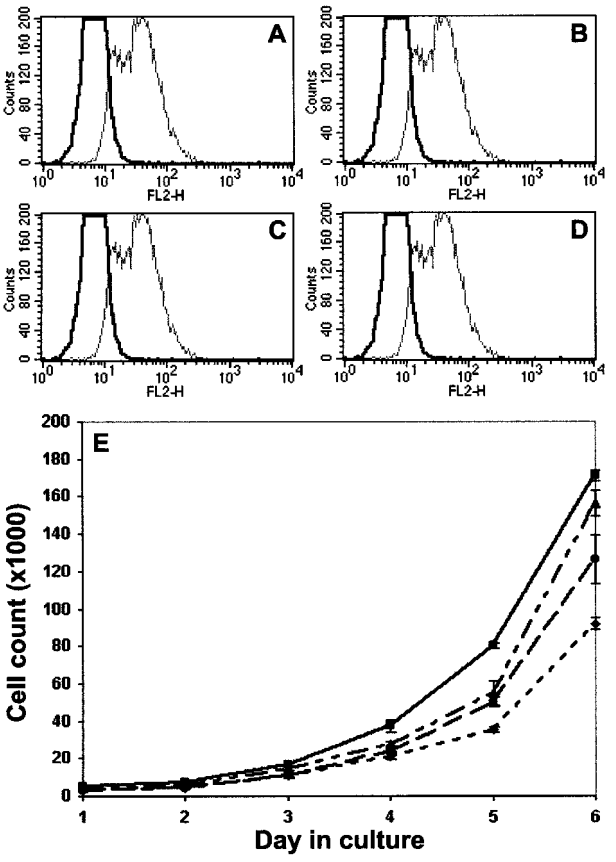

Figure 4. Apoptosis and intrinsic growth of HAS anti-sense cells in culture. **A–D:** Subconfluent cultures of tumor cell lines were trypsin released, washed, fixed, and permeabilized. Control aliquots of each cell suspension were incubated with 10 μg/ml of DNase. Apoptosis was measured by a TUNEL Red assay followed by two-color flow cytometry, gating on GFP-positive cells, and assessing incorporation of the red fluorophore in the FL-2 channel. **Black tracings** represent the FL-2 distribution of GFP (**A**), H2as (**B**), H3as (**C**), and H2/3as (**D**) cell lines. DNase control results are superimposed as **gray tracings**. **E:** Equivalent passages of each tumor cell line were plated in 48-well plates. At 24-hour intervals up to 6 days, quadruplicate wells of each cell line were trypsin released and manually counted in a hemacytometer. Growth curves are shown for GFP controls (**solid line**, **squares**), H2as (**dotted/dashed line**, **triangles**), H3as (**dashed line**, **circles**), H2/3as (**dotted line**, **diamonds**).

per five random sections of tumor ranged from 35 to 55% and was equivalent in all tumors. The high level of variability in these data among tumors derived from the same cell line suggested no HAS antisense-related trends. Hence, although intrinsic growth rate seemed to be significantly slowed in the HAS antisense-inhibited tumor cell lines, this did not account for the dramatic differences observed in tumor weight and volume.

Reduction of HA Synthesis Inhibits Angiogenesis

Visualized grossly on dissection, control tumors were obviously more vascularized than anti-sense HAS-expressing tumors. Furthermore, there is literature precedent for angiogenic regulation by HA. In particular, its oligomeric degradation products have been shown to mediate endothelial cell motility and proliferation.[28–30] To quantify vascularity, tumors were stained with a phycoerythrin-conjugated antibody to CD31, a vascular endothelial cell surface antigen. Representative grayscale sections of GFP control (Figure 5A) and H2/3as (Figure 5B) tumors illustrate differences in CD31 staining. Digital photographs of five random sections from each of three tumors per cell line were analyzed as TIF files in Adobe Photoshop.[27] Angiogenesis in PC3M-LN4 transfectant tumors is represented by average pixel density and normalized to untransfected control tumors (Figure 5C). Inhibition of HA synthesis in tumor cells reduced blood vessel density by 70 to 80%, despite insignificant differences in cellular density. Therefore, HA overproduction by tumor cells may be required for efficient subcutaneous growth because of its impact on angiogenesis.

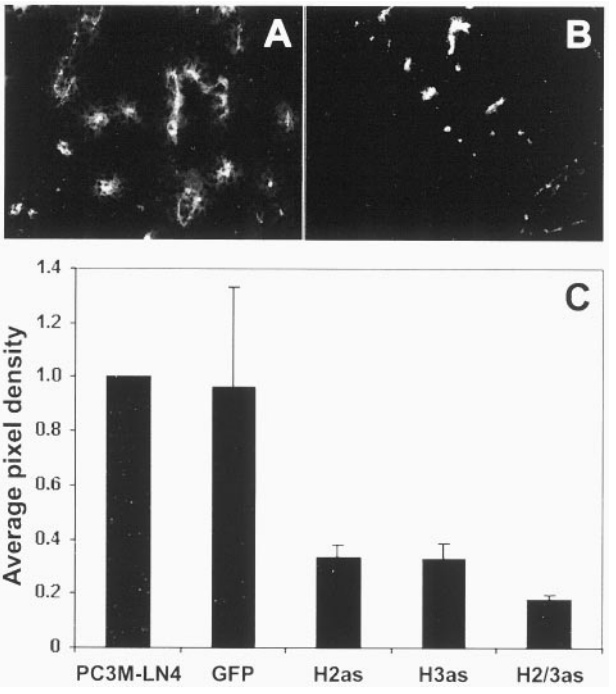

Figure 5. Antisense HAS expression in PC3M-LN4 cells yields poorly vascularized tumors relative to controls. CD31-phycoerythrin-conjugated antibody staining was used to quantify angiogenesis of tumor sections, visualized by fluorescence microscopy. Representative sections from GFP control (**A**) and HAS double antisense (**B**) tumors are shown. **C:** Five random sections from each of three tumors per cell line were digitally photographed and images processed as described in Materials and Methods. Average pixel density for each transfectant tumor section was then normalized to the average pixel density for untransfected PC3M-LN4 tumor sections.

Exogenous HA Restores Subcutaneous Tumor Growth and Vascular Density

If HA production were all that was required for efficient growth of PC3M-LN4 cells, then inclusion of excess quantities in the injection medium of the antisense-inhibited transfectants would be predicted to restore tumor growth kinetics to those of the control cells. Inclusion of 1 mg/ml of exogenous HA in the culture medium of untransfected, control, or HAS antisense-transfected PC3M-LN4 cells had no effect on the two-dimensional growth curves shown in Figure 4E (data not shown). To test this prediction *in vivo*, vector (GFP) and double antisense (H2/3as)-

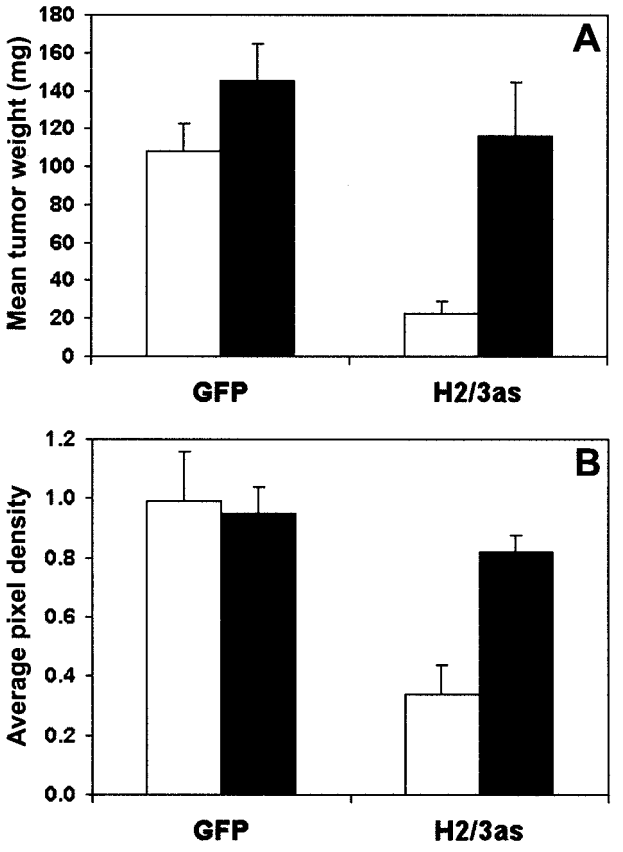

Figure 6. Exogenous HA restores control tumor growth kinetics and vascular density to double HAS antisense-inhibited PC3M-LN4 cells. **A:** Vector (GFP) and HAS double antisense (H2/3as)-transfected tumor cells were suspended in control culture medium (**white bars**) or medium containing 1 mg/ml of sodium hyaluronate (average size, 810 kd), and injected subcutaneously into the flanks of male SCID mice. Tumors were harvested and weighed after 3 weeks. Data are plotted as the mean wet weight (mg) ± SEM of seven to nine tumors per condition. **B:** CD31-phycoerythrin-conjugated antibody staining was used to quantify angiogenesis of tumor sections. Five random sections from each of three tumors per cell line injected in control medium (**white bars**) or HA-containing medium (**black bars**) were analyzed as described in Materials and Methods. Average pixel density of each section was normalized to that of untransfected PC3M-LN4 tumor sections.

transfected cells were suspended in standard medium (control) or medium containing 1 mg/ml of HA (average molecular weight, 810 kd) before subcutaneous injection as described. Tumors were harvested and weighed at 21 days (Figure 6A). Growth of control transfectants was slightly, but not significantly, stimulated by addition of HA to the injection medium. Inhibited growth of HAS double antisense cells, however, was enhanced to match growth of the controls. This confirmed the specific nature of the antisense inhibition and the requirement only for the product of the HAS isozymes, not for production by the tumor cell, retention at the surface by HAS, or expression of a specific isozyme.

The efficacy of growth restoration *in vivo*, but not in cultured cells, implies a more complex requirement for HA than to modify intrinsic growth rate of the cells, and is consistent with a putative role in angiogenesis. To investigate this possibility, we quantified vascular density of GFP control and H2/3as tumors injected in standard or HA-containing medium by CD31-phycoerythrin staining as described above. Average CD31-positive pixel density was comparable for GFP controls cells irrespective of injection medium (Figure 6B). However, the low vascular densities observed for H2/3as tumors injected in standard medium were entirely restored to control levels by addition of exogenous HA. This result provides direct support for the involvement of HA in tumor vascularization.

Discussion

Prostate cancer progression occurs with elevated HA deposition in the prostate stroma and tumor cell-associated HA is a bad prognostic factor. HA overproduction and cell surface retention correlates with malignant prostate tumor cell phenotype. In this report, we have used PC3M-LN4 aggressive prostate tumor cells selected for stable expression of antisense HAS constructs to assess the impact of inhibited HA production on tumorigenic behavior *in vivo*. Diminished HA synthesis resulting from reduced expression of either or both HAS enzyme isoforms significantly altered the growth kinetics of the tumor cells (75% reduction). Intrinsic proliferation and apoptosis in two-dimensional cell cultures were not sufficiently different to account for this observation. However, blood vessel densities within the HAS antisense-inhibited tumors reflected the same 75 to 80% reduction exhibited by tumor growth. These results strongly imply that the elevated HA levels produced by PC3M-LN4 cells function both to enhance cell growth within the tumor and to promote its vascularization.

Ample evidence exists for the function of HA in growth and development. HA is deposited in large quantities by cells undergoing mitosis, and facilitates both cell rounding and ultimate separation of the daughter cells.[3] Addition of HA to explanted embryonic mouse prostate tissue was required for ductal branching.[5] Targeted disruption of HAS2 is an embryonic lethal mutation in mice as a result of cessation in heart development.[4] Exogenous addition of HA to explanted heart tissue from these embryos was sufficient to restore wild-type levels of cardiac endothelial cell motility, functioning not only as a requisite migration substrate but also to influence transformation of the cells to a motile phenotype. The product of HAS enzymes, therefore, seems to be the essential component of these events. This is consistent with our observations that antisense HAS expression in PC3M-LN4 cells inhibits tumor growth and addition of HA to double antisense-inhibited cells restores their rate of tumor formation and vascularity to control levels. Although an essential component of growth, cells apparently do not need to make HA if it is made available to them.

Temporal and tissue-specific HA deposition has been implicated in normal growth, but also promotes pathological growth. HA overproduction by cultured cells has been shown to alleviate normal contact inhibited growth.[31] Addition of HA to explanted heart cells maintains them in an undifferentiated state, in which they retain tumor cell characteristics of motility and continued proliferation.[32] HA stimulates myeloma proliferation in

bone marrow, possibly by locally enhancing autocrine response to interleukin-6.[33] Specific relevance of HA biosynthetic enzymes to tumor growth has been demonstrated by HAS2 and HAS3 overexpression, both of which were shown to promote anchorage-independent growth,[22,34] and to enhance subcutaneous tumorigenicity in nude mice.[22,23] In some cases, HA involvement in tumorigenic behavior has been accompanied by altered motility and metastasis.[20,35–37] In the case of PC3M-LN4 subcutaneous tumors, there was no evidence of invasiveness or spontaneous metastasis either in control or in antisense HAS-inhibited tumors, suggesting altered motility is not a significant component of the tumorigenic mechanism of up-regulated HAS. It is more likely, therefore, that the observed differences in growth properties and tumor angiogenesis of the HAS antisense cells are modulating development of the tumors. As a corollary, metastasis of these cells in other models (ie, prostate orthotopic and intracardial injection[24]) may be promoted by the influence of HA in growth and vascularization at the remote site.

Interestingly, expression of antisense mRNA for HAS2 and HAS3 individually and in concert impacted tumor growth to the same extent. The most straightforward explanation for this phenomenon is that there is a requisite threshold of HA production that must be achieved or exceeded to effect control of growth or angiogenesis. In support of this, synthesis and secretion of HA were reduced differentially in all three HAS antisense transfectant cell lines, but cell surface HA was virtually unmeasurable by particle exclusion assay in any of the three lines.[26] Another possible explanation is a general disruption by antisense expression in the PC3M-LN4 cells. However, restored growth of tumors on augmentation of HA in the injection medium suggests this is not the case. It is also possible that there is nonspecific inhibition of both HAS2 and HAS3 by each respective antisense. The region selected for expression in antisense orientation, however, is the first 300 nucleotides of coding sequence, where the greatest differences in sequence alignment are manifest. Furthermore, reverse transcriptase-polymerase chain reaction amplification of HAS2 and HAS3 from the antisense-inhibited cells demonstrated specificity of message destabilization and quantification of HA synthesis indicated incomplete inhibition in the single antisense HAS cells. Collectively, these data support a threshold of HA synthesis that probably correlates to HA surface retention.

Several possible additional effects, which may be overlaid on this model, cannot be ruled out. First, there may be differential temporal regulation of the HAS isozymes necessary for cell division, which would be precluded by antisense expression. HAS2, for example, seems to be the most highly regulated isozyme, because gene regulation studies report no significant changes in the levels of HAS1 or HAS3 transcripts to various stimuli that impact HAS2.[6,38,39] In addition, although cells in culture and 21-day tumor sections failed to exhibit differences in apoptosis, absence of the requisite threshold on injection into the animals may initiate immediate cell death. This would diminish the original number of cells available to develop into a tumor, but would be undetected in our assay. HAS antisense-expressing cells could exhibit delayed initial growth rate, possibly as a result of reduced ability to stimulate angiogenesis, that would ultimately approach the rate of control cell growth. Preliminary experiments to determine the sacrifice endpoint for subcutaneous injection, in which the size of HAS antisense tumors no longer increased after 21 days (data not shown), argue against equivalent but delayed growth. Finally, the stably selected cells are a heterogeneous population that may still include a small percentage of HA-overproducing cells capable of growth. Abundance of cell surface HA has been hypothesized to envelope the cell in a semiorganized matrix that protects human gliomas[40] and also virulent strains of *Streptococcus pyogenes* bacteria[41] from cytotoxic killing mediated by natural killer cells in the bloodstream. SCID mice lack T and B cells, but retain natural killer cell activity, so antisense inhibition of surface HA may render PC3M-LN4 cells more susceptible to the vestiges of immune function in the animals. However, if this were the only mechanism of suppressed growth, the resultant tumors would be expected to be HA-rich and GFP-negative, suggesting this explanation also is incomplete.

Blood vessel densities of each antisense HAS permutation were decreased to a similar extent relative to controls, reflecting the effect observed in tumor growth kinetics. Because intrinsic differences in proliferation and apoptosis, both in cell cultures and in tumor sections, do not fully explain tumor size differential, it is likely that the postulated requisite tumor cell HA synthesis threshold directly impacts the ability of the cells to vascularize a developing tumor. Vessel density within the tumor was altered on a per-cell basis, not merely by a linear decrease with tumor size, suggesting direct impact of some factor produced by the tumor cell on endothelial recruitment. HAS3 overexpression has been correlated with increased blood vessel density in subcutaneous tumors,[23] but this is the first report of impaired HA production leading to decreased vascularization of a tumor. The role of HA, particularly of its oligosaccharides, in angiogenesis is well documented. Application of HA oligosaccharides has been shown to locally increase blood vessel density of rat skin.[30] HA oligo fractions extracted from rat ovaries were used to demonstrate the essential role of HA in ovarian neovascularization.[29] HA oligosaccharide products formed by hyaluronidase degradation of high-molecular weight HA was shown to stimulate blood vessel formation in a chick chorioallantoic membrane assay for angiogenesis.[42] Subsequently, the same group showed HA oligos specifically mediated endothelial cell proliferation and recruitment, while high-molecular weight HA was actually anti-proliferative,[28] suggested elevated HA in tumors appeared to correlate with angiogenesis,[43] and that molecular weight differences in HA were mediated by cells within the tumor.[44] Tumor cells may therefore benefit from the presence of HA polymer either by stimulating or exploiting existing hyaluronidase activity within the tissue they are invading, or by expressing it themselves. In fact, overexpression of hyaluronidase in gliomas has been correlated to angiogenesis,[45] and im-

munohistological data suggest this may occur in prostate carcinoma, because the hyaluronidase isoform Hyal-1 was shown to be overexpressed during human cancer progression concurrently with elevated HA deposition.[15]

Our data are consistent with a model in which tumor cells with enhanced capacity to synthesize and retain pericellular HA are surrounded by a hydrated envelope that facilitates tumorigenicity, perhaps by altering the composition and interfering with the integrity of tissue stromal matrices or permitting the tumor cells to evade immune system detection. Short HA oligosaccharides that stimulate angiogenesis may be elevated in the environs of such tumor cells through the action of hyaluronidase enzymes. Inhibition of HAS enzyme expression within the tumor would then decrease vascularization by eliminating production of this angiogenic stimulus and thereby suppress tumor growth. HA oligos may also facilitate motility and inappropriate proliferation in autocrine manner by signal transduction through tumor cell HA receptors such as CD44 and RHAMM.[46]

Acknowledgments

We thank Dr. Sundaram Ramakrishnan for expert advice and assistance with angiogenesis quantification, Dr. Ted Oegema and Dr. Joseph Barycki for many thoughtful discussions, and Dr. Leo Furcht for ongoing supportive input.

References

1. Landis SH, Murray T, Bolden S, Wingo PA: Cancer statistics, 1999. CA Cancer J Clin 1999, 49:8–31
2. Fraser JR, Laurent TC, Laurent UB: Hyaluronan: its nature, distribution, functions and turnover. J Intern Med 1997, 242:27–33
3. Evanko SP, Angello JC, Wight TN: Formation of hyaluronan- and versican-rich pericellular matrix is required for proliferation and migration of vascular smooth muscle cells. Arterioscler Thromb Vasc Biol 1999, 19:1004–1013
4. Camenisch TD, Spicer AP, Brehm-Gibson T, Biesterfeldt J, Augustine ML, Calabro Jr A, Kubalak S, Klewer SE, McDonald JA: Disruption of hyaluronan synthase-2 abrogates normal cardiac morphogenesis and hyaluronan-mediated transformation of epithelium to mesenchyme. J Clin Invest 2000, 106:349–360
5. Gakunga P, Frost G, Shuster S, Cunha G, Formby B, Stern R: Hyaluronan is a prerequisite for ductal branching morphogenesis. Development 1997, 124:3987–3997
6. Yung S, Thomas GJ, Davies M: Induction of hyaluronan metabolism after mechanical injury of human peritoneal mesothelial cells in vitro. Kidney Int 2000, 58:1953–1962
7. Auvinen P, Tammi R, Parkkinen J, Tammi M, Agren U, Johansson R, Hirvikoski P, Eskelinen M, Kosma VM: Hyaluronan in peritumoral stroma and malignant cells associates with breast cancer spreading and predicts survival. Am J Pathol 2000, 156:529–536
8. Bohm J, Niskanen L, Tammi R, Tammi M, Eskelinen M, Pirinen R, Hollmen S, Alhava E, Kosma VM: Hyaluronan expression in differentiated thyroid carcinoma. J Pathol 2002, 196:180–185
9. Anttila MA, Tammi RH, Tammi MI, Syrjanen KJ, Saarikoski SV, Kosma VM: High levels of stromal hyaluronan predict poor disease outcome in epithelial ovarian cancer. Cancer Res 2000, 60:150–155
10. Ropponen K, Tammi M, Parkkinen J, Eskelinen M, Tammi R, Lipponen P, Agren U, Alhava E, Kosma VM: Tumor cell-associated hyaluronan as an unfavorable prognostic factor in colorectal cancer. Cancer Res 1998, 58:342–347
11. Lokeshwar VB, Obek C, Soloway MS, Block NL: Tumor-associated hyaluronic acid: a new sensitive and specific urine marker for bladder cancer [published erratum appears in Cancer Res 1998, 58:3191]. Cancer Res 1997, 57:773–777
12. De Klerk DP: The glycosaminoglycans of normal and hyperplastic prostate. Prostate 1983, 4:73–81
13. De Klerk DP, Lee DV, Human HJ: Glycosaminoglycans of human prostatic cancer. J Urol 1984, 131:1008–1012
14. Lipponen P, Aaltomaa S, Tammi R, Tammi M, Agren U, Kosma VM: High stromal hyaluronan level is associated with poor differentiation and metastasis in prostate cancer. Eur J Cancer 2001, 37:849–856
15. Lokeshwar VB, Rubinowicz D, Schroeder GL, Forgacs E, Minna JD, Block NL, Nadji M, Lokeshwar BL: Stromal and epithelial expression of tumor markers hyaluronic acid and HYAL1 hyaluronidase in prostate cancer. J Biol Chem 2001, 276:11922–11932
16. Weigel PH, Hascall VC, Tammi M: Hyaluronan synthases. J Biol Chem 1997, 272:13997–14000
17. Shyjan AM, Heldin P, Butcher EC, Yoshino T, Briskin MJ: Functional cloning of the cDNA for a human hyaluronan synthase. J Biol Chem 1996, 271:23395–23399
18. Watanabe K, Yamaguchi Y: Molecular identification of a putative human hyaluronan synthase. J Biol Chem 1996, 271:22945–22948
19. Spicer AP, McDonald JA: Characterization and molecular evolution of a vertebrate hyaluronan synthase gene family. J Biol Chem 1998, 273:1923–1932
20. Brinck J, Heldin P: Expression of recombinant hyaluronan synthase (HAS) isoforms in CHO cells reduces cell migration and cell surface CD44. Exp Cell Res 1999, 252:342–351
21. Itano N, Sawai T, Yoshida M, Lenas P, Yamada Y, Imagawa M, Shinomura T, Hamaguchi M, Yoshida Y, Ohnuki Y, Miyauchi S, Spicer AP, McDonald JA, Kimata K: Three isoforms of mammalian hyaluronan synthases have distinct enzymatic properties. J Biol Chem 1999, 274:25085–25092
22. Kosaki R, Watanabe K, Yamaguchi Y: Overproduction of hyaluronan by expression of the hyaluronan synthase Has2 enhances anchorage-independent growth and tumorigenicity. Cancer Res 1999, 59:1141–1145
23. Liu N, Gao F, Han Z, Xu X, Underhill CB, Zhang L: Hyaluronan synthase 3 overexpression promotes the growth of TSU prostate cancer cells. Cancer Res 2001, 61:5207–5214
24. Pettaway CA, Pathak S, Greene G, Ramirez E, Wilson MR, Killion JJ, Fidler IJ: Selection of highly metastatic variants of different human prostatic carcinomas using orthotopic implantation in nude mice. Clin Cancer Res 1996, 2:1627–1636
25. Simpson MA, Reiland J, Burger SR, Furcht LT, Spicer AP, Oegema Jr TR, McCarthy JB: Hyaluronan synthase elevation in metastatic prostate carcinoma cells correlates with hyaluronan surface retention, a prerequisite for rapid adhesion to bone marrow endothelial cells. J Biol Chem 2001, 276:17949–17957
26. Simpson MA, Wilson CM, Furcht LT, Spicer AP, Oegema Jr TR, McCarthy JB: Manipulation of hyaluronan synthase expression in prostate adenocarcinoma cells alters pericellular matrix retention and adhesion to bone marrow endothelial cells. J Biol Chem 2002, 277:10050–10057
27. Wild R, Ramakrishnan S, Sedgewick J, Griffioen AW: Quantitative assessment of angiogenesis and tumor vessel architecture by computer-assisted digital image analysis: effects of VEGF-toxin conjugate on tumor microvessel density. Microvasc Res 2000, 59:368–376
28. West DC, Kumar S: The effect of hyaluronate and its oligosaccharides on endothelial cell proliferation and monolayer integrity. Exp Cell Res 1989, 183:179–196
29. Sato E, Miyamoto H, Koide SS: Hyaluronic acid-like substance from mouse ovaries with angiogenic activity. Z Naturforsch [C] 1990, 45:873–880
30. Sattar A, Rooney P, Kumar S, Pye D, West DC, Scott I, Ledger P: Application of angiogenic oligosaccharides of hyaluronan increases blood vessel numbers in rat skin. J Invest Dermatol 1994, 103:576–579
31. Itano N, Atsumi F, Sawai T, Yamada Y, Miyaishi O, Senga T, Hamaguchi M, Kimata K: Abnormal accumulation of hyaluronan matrix diminishes contact inhibition of cell growth and promotes cell migration. Proc Natl Acad Sci USA 2002, 99:3609–3614
32. Iocono JA, Bisignani GJ, Krummel TM, Ehrlich HP: Inhibiting the differentiation of myocardiocytes by hyaluronic acid. J Surg Res 1998, 76:111–116

33. Vincent T, Jourdan M, Sy MS, Klein B, Mechti N: Hyaluronic acid induces survival and proliferation of human myeloma cells through an interleukin-6-mediated pathway involving the phosphorylation of retinoblastoma protein. J Biol Chem 2001, 276:14728–14736
34. Li Y, Heldin P: Hyaluronan production increases the malignant properties of mesothelioma cells. Br J Cancer 2001, 85:600–607
35. Dube B, Luke HJ, Aumailley M, Prehm P: Hyaluronan reduces migration and proliferation in CHO cells. Biochim Biophys Acta 2001, 1538:283–289
36. Itano N, Sawai T, Miyaishi O, Kimata K: Relationship between hyaluronan production and metastatic potential of mouse mammary carcinoma cells. Cancer Res 1999, 59:2499–2504
37. Yu Q, Toole BP, Stamenkovic I: Induction of apoptosis of metastatic mammary carcinoma cells in vivo by disruption of tumor cell surface CD44 function. J Exp Med 1997, 186:1985–1996
38. Jacobson A, Brinck J, Briskin MJ, Spicer AP, Heldin P: Expression of human hyaluronan synthases in response to external stimuli. Biochem J 2000, 348:29–35
39. Zhang W, Watson CE, Liu C, Williams KJ, Werth VP: Glucocorticoids induce a near-total suppression of hyaluronan synthase mRNA in dermal fibroblasts and in osteoblasts: a molecular mechanism contributing to organ atrophy. Biochem J 2000, 349:91–97
40. Gately CL, Muul LM, Greenwood MA, Papazoglou S, Dick SJ, Kornblith PL, Smith BH, Gately MK: In vitro studies on the cell-mediated immune response to human brain tumors. II. Leukocyte-induced coats of glycosaminoglycan increase the resistance of glioma cells to cellular immune attack. J Immunol 1984, 133:3387–3395
41. Cywes C, Wessels MR: Group A Streptococcus tissue invasion by CD44-mediated cell signalling. Nature 2001, 414:648–652
42. West DC, Hampson IN, Arnold F, Kumar S: Angiogenesis induced by degradation products of hyaluronic acid. Science 1985, 228:1324–1326
43. West DC, Kumar S: Tumour-associated hyaluronan: a potential regulator of tumour angiogenesis. Int J Radiat Biol 1991, 60:55–60
44. Rooney P, Kumar S, Ponting J, Wang M: The role of hyaluronan in tumour neovascularization (review). Int J Cancer 1995, 60:632–636
45. Liu D, Pearlman E, Diaconu E, Guo K, Mori H, Haqqi T, Markowitz S, Willson J, Sy MS: Expression of hyaluronidase by tumor cells induces angiogenesis in vivo. Proc Natl Acad Sci USA 1996, 93:7832–7837
46. Turley EA, Noble PW, Bourguignon LY: Signaling properties of hyaluronan receptors. J Biol Chem 2002, 277:4589–4592